https://doi.org/10.1038/s41592-024-02188-8

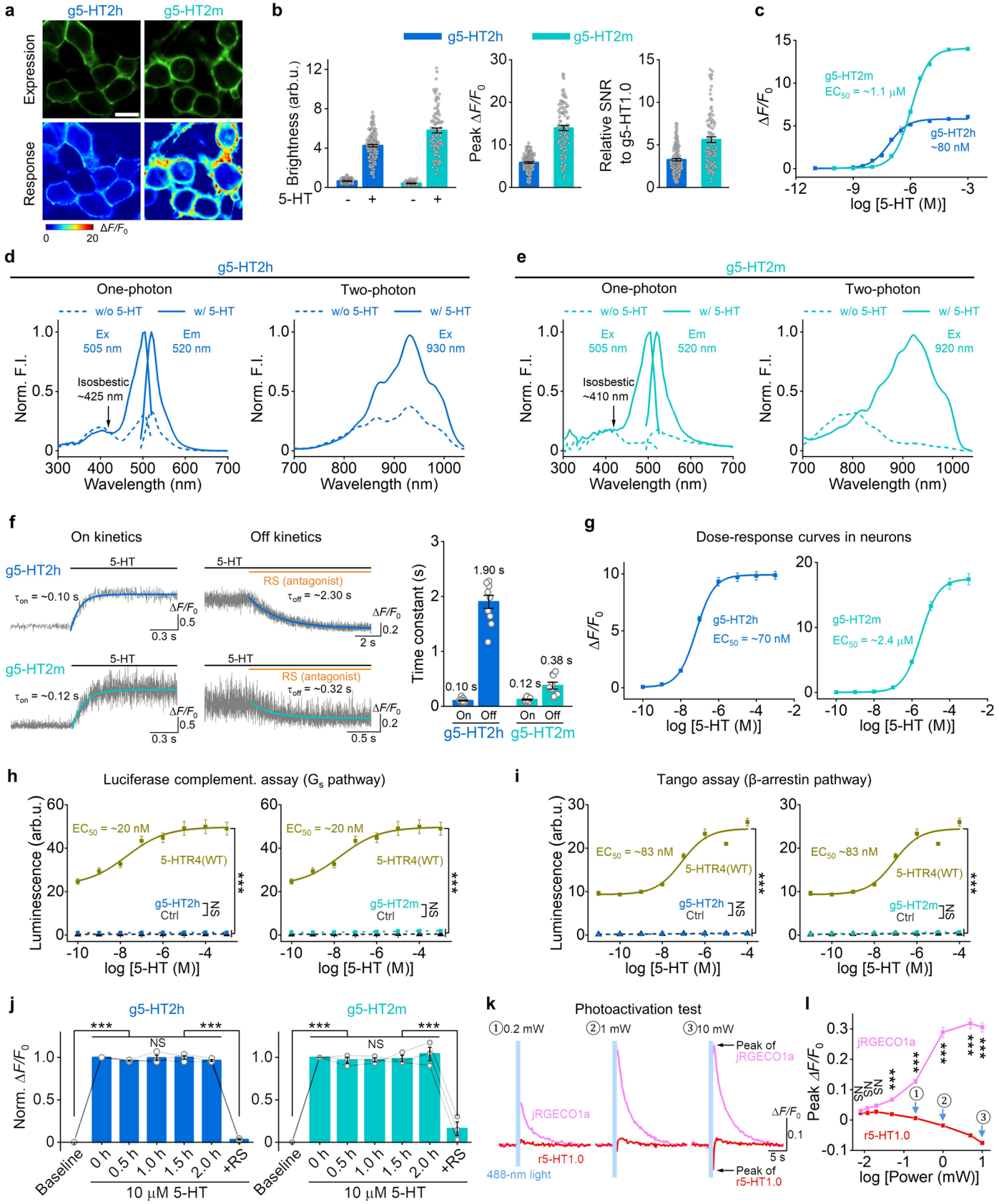

Extended Data Fig. 1 | See next page for caption.

https://doi.org/10.1038/s41592-024-02188-8

Extended Data Fig. 1 | Characterization of GRAB$_{5\text{-}HT}$ sensors in HEK293T cells and cultured rat cortical neurons. a, Representative images showing the expression (top, with 5-HT) and responses (bottom) to 100 μM 5-HT for g5-HT2h (left) and g5-HT2m (right). Scale bar, 20 μm. **b**, The group summary of the brightness (left), peak $\Delta F/F_0$ (middle) and SNR (right) of g5-HT2h and g5-HT2m. The SNR is relative to g5-HT1.0; arb.u., arbitrary units. $n = 154$ cells from 3 coverslips (short for 154/3) for g5-HT2h, 98/3 for g5-HT2m. **c**, Dose-dependent curves of g5-HT2h and g5-HT2m. $n = 3$ wells for each sensor with 300–500 cells per well. **d**–**e**, Excitation (Ex) and emission (Em) spectra of g5-HT2h (**d**) and g5-HT2m (**e**) in the absence (dash line) and presence of 10 μM 5-HT (solid line) under one-photon (left), and two-photon excitation (right). w/o, without; w/, with. **f**, Representative traces of sensor fluorescence increase to 5-HT puffing and decrease to RS puffing (left). Group summary of on and off kinetics (right). $n = 16$ cells from 4 coverslips (16/4) for g5-HT2h on kinetics, 10/3 for g5-HT2h off kinetics, 11/3 for g5-HT2m on kinetics, 9/3 for g5-HT2m off kinetics. **g**, Dose-response curves of g5-HT2h (left) and g5-HT2m (right) in cultured rat cortical neurons. $n = 60$ ROIs from 3 coverslips for g5-HT2h and g5-HT2m. **h**–**i**, Downstream coupling tests of g5-HT2h and g5-HT2m for G_s coupling (**h**) and β-arrestin coupling (**i**). Data of WT and Ctrl groups were replotted from Fig. 2l. $n = 3$ wells per group with 200–500 cells per well. One-way ANOVA followed by Tukey's multiple-comparison tests, in panel **h**, post hoc test in 1 mM 5-HT: $P = 2.65 \times 10^{-6}$ and 0.96 for g5-HT2h versus WT and Ctrl, respectively, $P = 2.93 \times 10^{-6}$ and 0.82 for g5-HT2m versus WT and Ctrl, respectively; in panel **i**, post hoc test: $P = 4.94 \times 10^{-8}$ and 1 for g5-HT2h versus WT and Ctrl, respectively, $P = 5.96 \times 10^{-8}$ and 0.88 for g5-HT2m versus WT and Ctrl, respectively. **j**, The fluorescence of g5-HT2h (left) and g5-HT2m (right) expressed in cultured rat cortical neurons in response to a 2-h application of 5-HT, followed by RS. $n = 3$ wells for each sensor. One-way repeated measures ANOVA followed by Tukey's multiple-comparison tests, for g5-HT2h, $F = 670$, $P = 2.83 \times 10^{-5}$, post hoc test: $P = 0$ for baseline versus 0 h, $P = 0$ for 2.0 h versus RS, $P = 0.76, 1, 1, 0.80$ for 0 h versus 0.5 h, 1 h, 1.5 h or 2.0 h, respectively; for 5-HT2m, $F = 100.3$, $P = 0.006$, post hoc test: $P = 1.13 \times 10^{-6}$ for baseline versus 0 h, $P = 1.77 \times 10^{-7}$ for 2.0 h versus RS, $P = 1, 1, 1, 0.99$ for 0 h versus 0.5 h, 1 h, 1.5 h or 2.0 h, respectively. **k**, Averaged traces of jRGECO1a and r5-HT1.0 in response to 0.2, 1 and 10-mW blue light, respectively. **l**, Blue light intensity-dependent peak $\Delta F/F_0$ curves of jRGECO1a or r5-HT1.0. $n = 37/2$ for jRGECO1a and 49/2 for r5-HT1.0 in **k**, **l**. Two-way ANOVA followed by Tukey's multiple-comparison tests, for jRGECO1a versus r5-HT1.0 under indicated blue light power, $P = 1, 0.9761, 0.8783, 5.22 \times 10^{-4}, 0, 0, 0$ and 0, respectively. Data are shown as mean ± s.e.m. in **b**,**c**,**f**–**l**, with the error bars indicating the s.e.m. $^{***}P < 0.001$, n.s., not significant.

https://doi.org/10.1038/s41592-024-02188-8

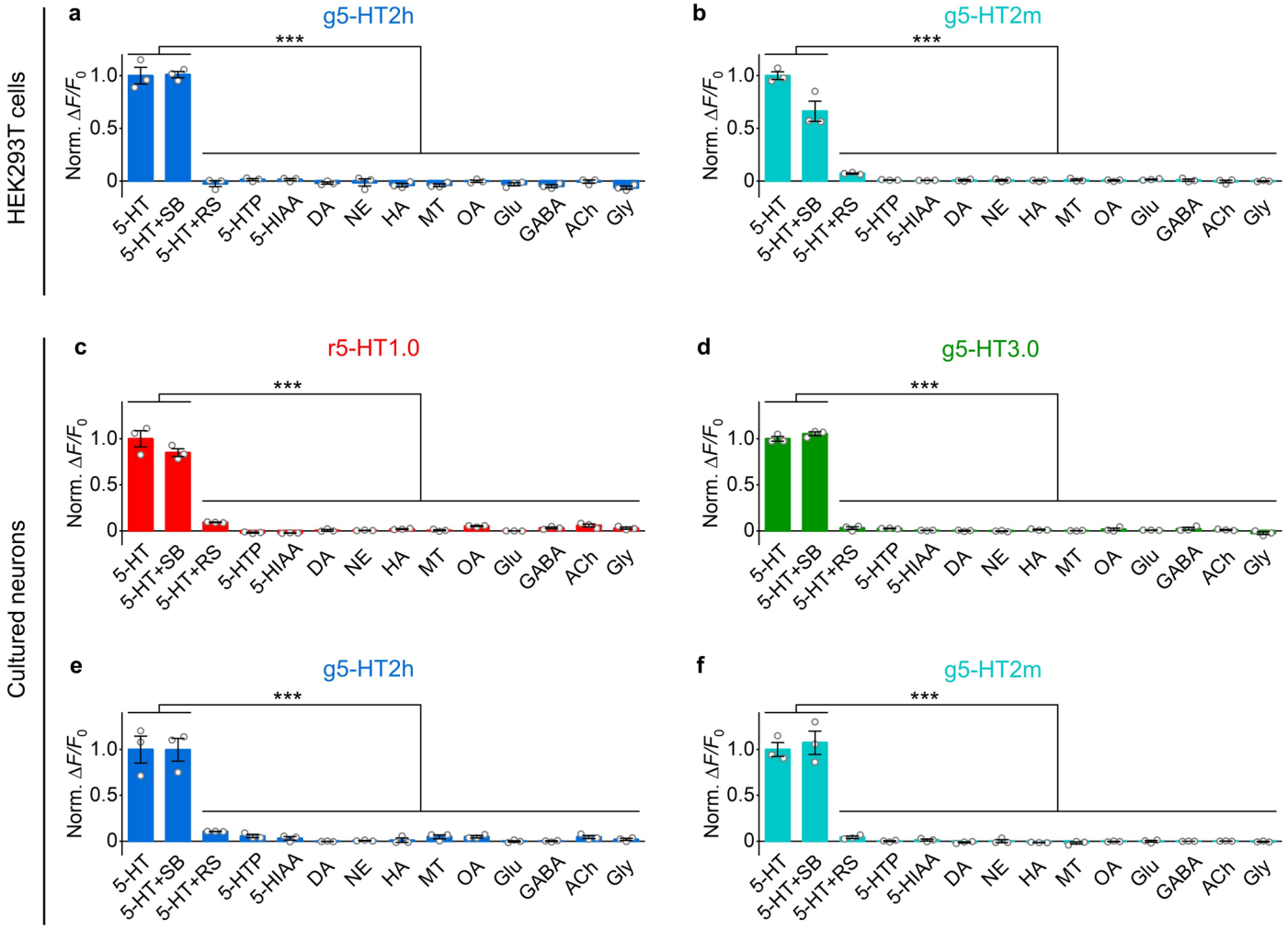

Extended Data Fig. 2 | Specificity of 5-HT sensors. Specificity test of indicated sensors in HEK293T cells (**a, b**) or cultured rat cortical neurons (**c**–**f**) to 5-HT alone, 5-HT together with SB, 5-HT together with RS, and 5-HT precursor, 5-HT metabolites, as well as other neurotransmitters and neuromodulators (all compounds at 10 μM except RS at 100 μM). 5-HTP, 5-hydroxytryptophan; 5-HIAA, 5-hydroxyindole acetic acid; DA, dopamine; NE, norepinephrine; HA, histamine; MT, melatonin; OA, octopamine; Glu, glutamate; GABA, gamma-aminobutyric acid; ACh, acetylcholine; Gly, glycine. Norm., normalized. $n = 3$ wells for each group with 200–500 cells per well. One-way ANOVA followed by Tukey's multiple-comparison tests, in panel **a**, $F_{13,28} = 180.2$, $P = 2.08 \times 10^{-23}$, post hoc test: $P = 0$ for 5-HT versus 5-HT and RS, and other compounds; in panel **b**, $F_{13,28} = 120$, $P = 5.52 \times 10^{-21}$, post hoc test: $P = 0$ for 5-HT versus 5-HT and RS, and other compounds; in panel **c**, $F_{13,28} = 148.9$, $P = 2.86 \times 10^{-22}$, post hoc test: $P = 0$ for 5-HT versus 5-HT and RS, and other compounds; in panel **d**, $F_{13,28} = 918$, $P = 3.16 \times 10^{-33}$, post hoc test: $P = 0$ for 5-HT versus 5-HT and RS, and other compounds; in panel **e**, $F_{13,28} = 44.2$, $P = 3.65 \times 10^{-15}$, post hoc test: $P = 4.39 \times 10^{-7}$, 2.06×10^{-7}, 9.18×10^{-8}, 1.26×10^{-7}, 1.26×10^{-7}, 1.26×10^{-7}, 2.08×10^{-7}, 2.08×10^{-7}, 1.26×10^{-7}, 1.26×10^{-7}, 2.09×10^{-7} and 9.18×10^{-8} for 5-HT versus 5-HT and RS, and 5-HTP, 5-HIAA, DA, NE, HA, MT, OA, Glu, GABA, ACh and Gly; in panel **f**, $F_{13,28} = 87.9$, $P = 3.83 \times 10^{-19}$, post hoc test: $P = 1.75 \times 10^{-9}$, 0, 2.33×10^{-11}, 0, 0, 0, 0, 0, 0, 0 and 0 for 5-HT versus 5-HT and RS, and 5-HTP, 5-HIAA, DA, NE, HA, MT, OA, Glu, GABA, ACh and Gly. Data are shown as mean ± s.e.m., with the error bars indicating the s.e.m. ***$P < 0.001$.

https://doi.org/10.1038/s41592-024-02188-8

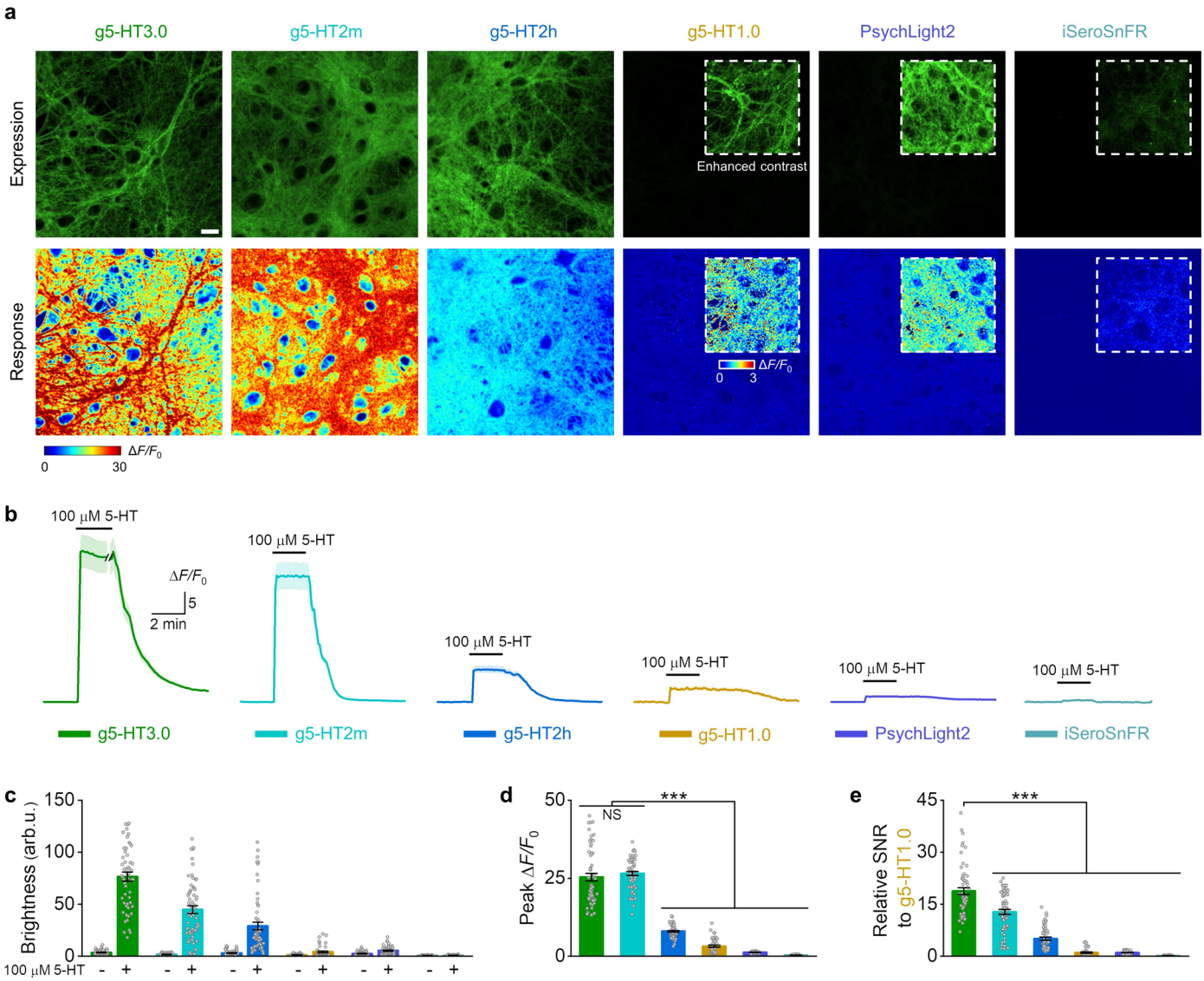

Extended Data Fig. 3 | Comparison of single GFP-based 5-HT sensors in cultured rat cortical neurons. a, Representative images showing the fluorescence expression (top) and responses (bottom) to 100 μM 5-HT for different sensors as indicated. Insets with white dashed outlines in images have either enhanced contrast (top) or different pseudocolor scales (bottom). Similar results were observed for more than 30 neurons. Scale bar, 20 μm. **b**, Representative traces in response to 100 μM 5-HT for different sensors as indicated. **c**–**e**, Group summary of the brightness (**c**), peak ΔF/F_0 (**d**) and SNR (**e**). The SNR of all sensors is relative to the SNR of g5-HT1.0; arb.u., arbitrary units, the basal brightness of g5-HT1.0 was set to 1. $n = 56$ ROIs from 3 coverslip (short for 56/3) for g5-HT3.0, 60/3 for g5-HT2m, 60/3 for g5-HT2h, 48/3 for g5-HT1.0, 60/3 for PsychLight2 and 60/3 for iSeroSnFR. One-way ANOVA followed by Tukey's multiple-comparison tests for **d**,**e**. For peak ΔF/F_0 in **d**, $F_{5,338} = 446.9$, $P = 1.46 \times 10^{-146}$, post hoc test: $P = 0.696$, 7.75×10^{-9}, 1.01×10^{-8}, 0 and 0 for g5-HT3.0 versus g5-HT2m, g5-HT2h, g5-HT1.0, PsychLight2 and iSeroSnFR; $P = 8.8 \times 10^{-9}$, 1.6×10^{-8}, 0 and 2.49×10^{-8} for g5-HT2m versus g5-HT2h, g5-HT1.0, PsychLight2 and iSeroSnFR. For relative SNR in **e**, $F_{5,338} = 195.1$, $P = 2.46 \times 10^{-97}$, post hoc test: $P = 7.55 \times 10^{-9}$, 0, 7.92×10^{-9}, 8.66×10^{-9} and 6.64×10^{-8} for g5-HT3.0 versus g5-HT2m, g5-HT2h, g5-HT1.0, PsychLight2 and iSeroSnFR. Data are shown as mean ± s.e.m. in **b**–**e**, with the error bars or shaded regions indicating the s.e.m. ***$P < 0.001$, n.s., not significant.

https://doi.org/10.1038/s41592-024-02188-8

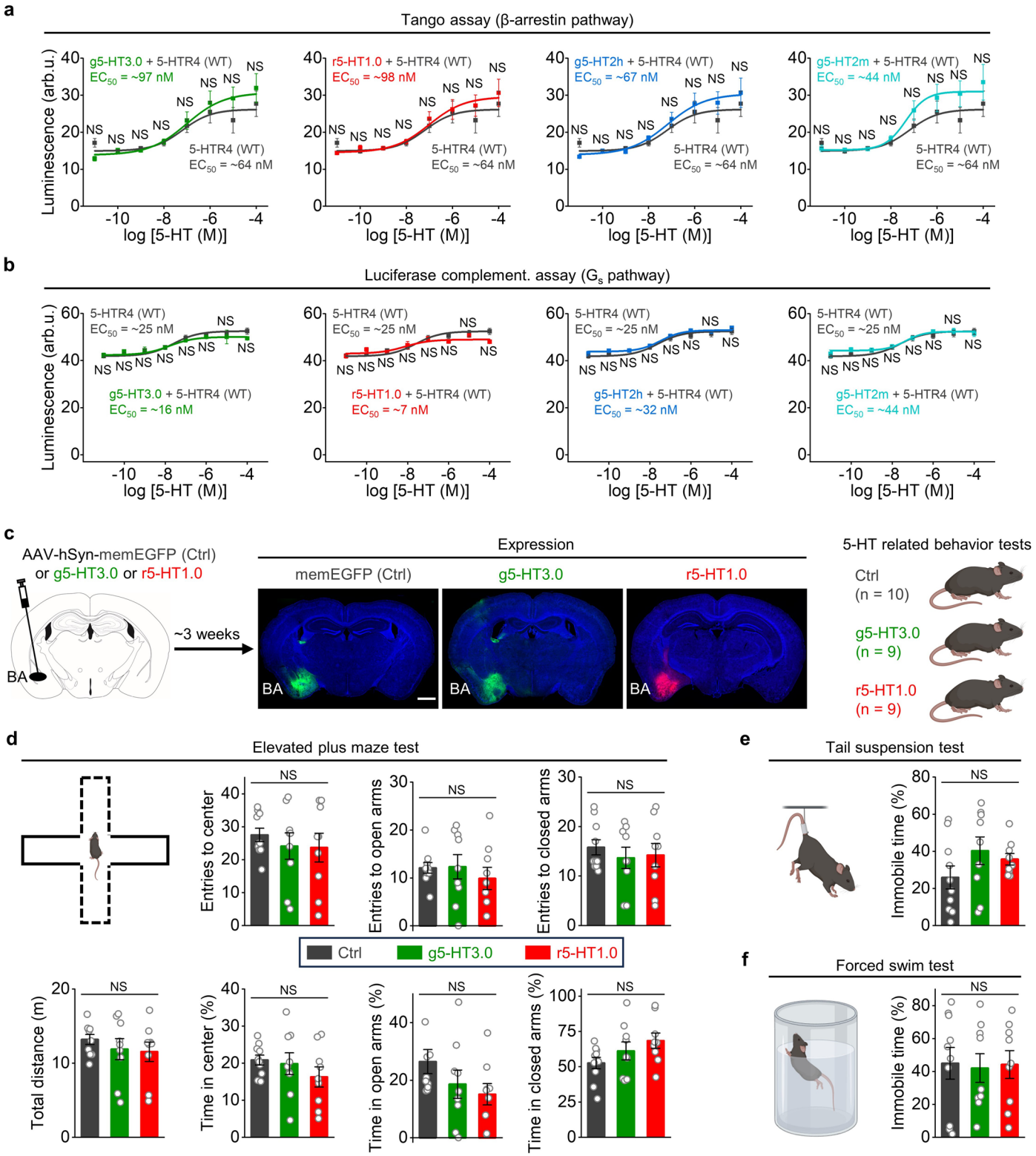

Extended Data Fig. 4 | See next page for caption.

https://doi.org/10.1038/s41592-024-02188-8

Extended Data Fig. 4 | Expression of GRAB$_{5\text{-HT}}$ sensors shows minimal buffering effects. a–**b**, *In vitro* test of buffering effects according to downstream coupling tests for β-arrestin coupling (**a**) and G_s coupling (**b**). $n = 9$ wells from three independent cultures per group with 200–500 cells per well. WT, wild type (the same WT results were used for different sensors in each assay); arb.u., arbitrary units. Two-way ANOVA tests were performed followed by Tukey's multiple-comparison tests. In panel **a**, for g5-HT3.0 + 5-HTR4 versus 5-HTR4 only, $P = 0.9877, 1, 1, 1, 1, 1, 0.8698$ and 0.9888 in the application of 5-HT concentration from 10^{-11} to 10^{-4} M, respectively; for r5-HT1.0 + 5-HTR4 versus 5-HTR4 only, $P = 0.9999, 1, 1, 1, 1, 1, 0.9929$ and 0.9996; for g5-HT2h + 5-HTR4 versus 5-HTR4 only, $P = 0.9956, 1, 1, 1, 1, 1, 0.9722$ and 0.9997; for g5-HT2m + 5-HTR4 versus 5-HTR4 only, $P = 1, 1, 1, 1, 0.9968, 0.9987, 0.7619$ and 0.9252. In panel **b**, for g5-HT3.0 + 5-HTR4 versus 5-HTR4 only, $P = 1, 1, 1, 1, 1, 1, 1$ and 0.8968; for r5-HT1.0 + 5-HTR4 versus 5-HTR4 only, $P = 1, 0.9755, 1, 1, 1, 0.9177, 1$ and 0.104; for g5-HT2h + 5-HTR4 versus 5-HTR4 only, $P = 1, 0.9972, 1, 1, 1, 0.9349, 1$ and 0.9984; for g5-HT2m + 5-HTR4 versus 5-HTR4 only, $P = 1, 0.9906, 1, 1, 1, 0.9981, 1$ and 1. **c**–**f**, *In vivo* test of buffering effects using multiple 5-HT related behavior tests. $n = 10, 9$ and 9 mice for the Ctrl, g5-HT3.0 and r5-HT1.0 group, respectively. **c**, Schematic illustrates the AAV injections of memEGFP (control) or g5-HT3.0 or r5-HT1.0 in mice basal amygdala (BA) (left); representative images exhibit the corresponding expression, scale bar, 1 mm (middle); cartoon shows mice for 5-HT related behavior tests (right). **d**–**f**, Schematic illustration (left) and quantification of behavioral parameters (right) in the elevated plus maze test (**d**), the tail suspension test (**e**) and the forced swim test (**f**). One-way ANOVA tests were performed. In panel **d**, $F_{2,25} = 0.366$, $P = 0.6975$ for entries to center; $F_{2,25} = 0.433$, $P = 0.6534$ for entries to open arms; $F_{2,25} = 0.3078$, $P = 0.7378$ for entries to closed arms; $F_{2,25} = 0.5944$, $P = 0.5595$ for total distance; $F_{2,25} = 1.0191$, $P = 0.3754$ for time in center; $F_{2,25} = 1.8749$, $P = 0.1743$ for time in open arms; $F_{2,25} = 2.3079$, $P = 0.1203$ for time in closed arms. In panel **e**, $F_{2,25} = 1.5753$, $P = 0.2268$. In panel **f**, $F_{2,25} = 0.0281$, $P = 0.9723$. Data are shown as mean ± s.e.m. in **a**–**b**, **d**–**f**, with the error bars indicating the s.e.m. n.s., not significant.

https://doi.org/10.1038/s41592-024-02188-8

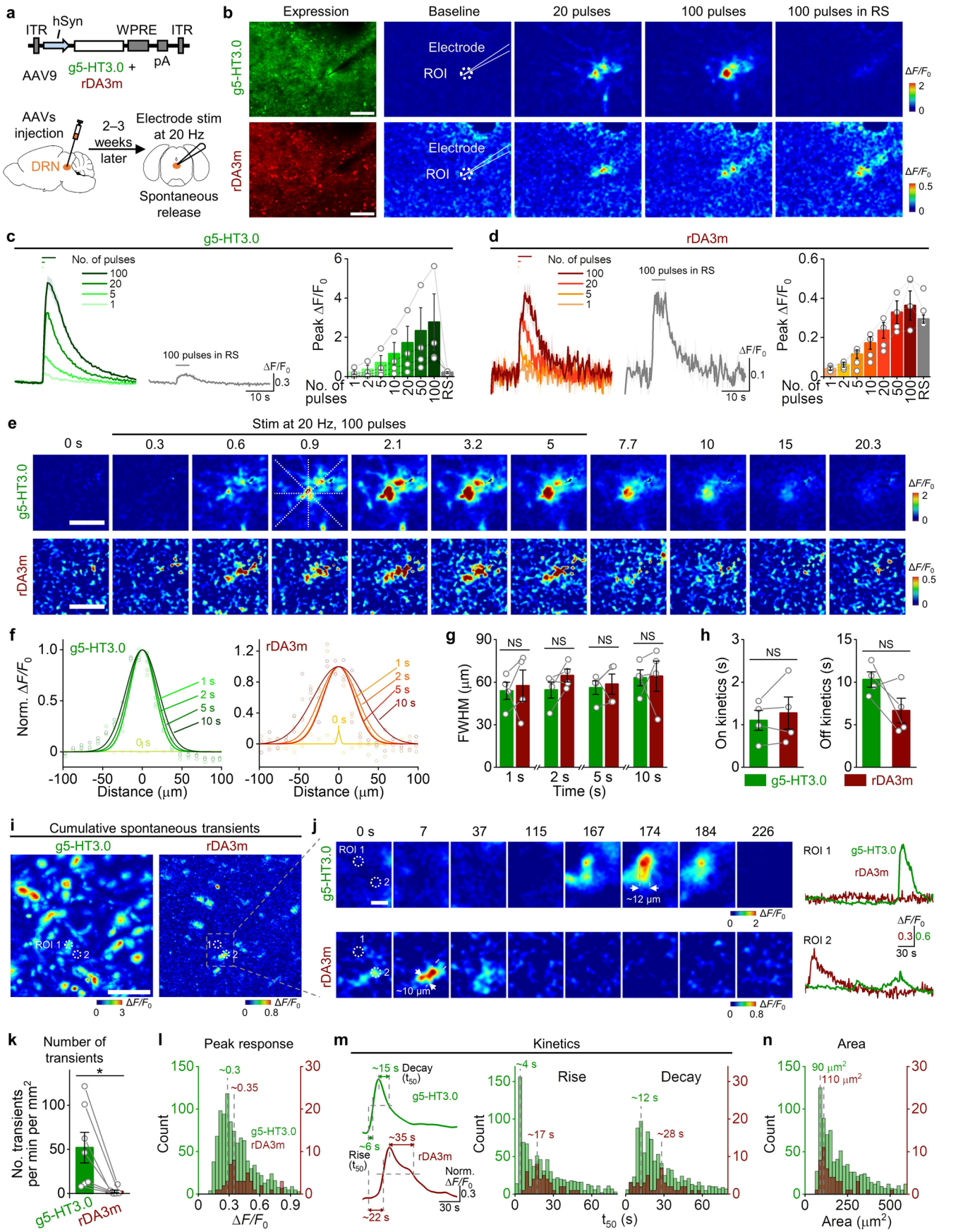

Extended Data Fig. 5 | See next page for caption.

https://doi.org/10.1038/s41592-024-02188-8

Extended Data Fig. 5 | Dual-color imaging of 5-HT and DA dynamics in acute mouse brain slices with high spatial-temporal resolution. a, Schematic illustrates the mouse brain slice experiments. **b**–**h**, Electrical stimulation evoked 5-HT and DA release. **b**, Representative fluorescence and pseudocolor images of g5-HT3.0 (top) and rDA3m (bottom) at baseline and in response to the indicated electrical stimuli, in the presence of artificial cerebrospinal fluid (ACSF) or 100 μM RS. Similar results were observed for 4 slices. The white dashed circle (50 μm in diameter) indicates the ROI used for further analysis; the white line indicates the stimulating electrode location. Scale bar, 100 μm. **c**–**d**, Representative traces and summary data for changes in g5-HT3.0 (**c**) and rDA3m (**d**) fluorescence in response to the indicated stimuli in ACSF or RS. **e**, Example time-lapse pseudocolor images of g5-HT3.0 (top) and rDA3m (bottom) in response to indicated electrical stimuli. Similar results were observed for 4 slices. The dashed lines were used to analyze spatial and temporal dynamics; image averaged from three trials conducted in one slice. Scale bar, 100 μm. **f**, Example spatial dynamics of the fluorescence changes shown in (**e**). **g**, Summary of the full width at half maximum (FWHM) of activity-dependent 5-HT and DA signals measured in **f** at the indicated time points. Two-tailed paired *t*-tests, $P = 0.7559$, 0.1318, 0.741 and 0.9301 for 1 s, 2 s, 5 s and 10 s, respectively. **h**, Group summary of on and off kinetics for the 100-pulse evoked response of g5-HT3.0 and rDA3m. Two-tailed paired *t*-tests, $P = 0.4308$ and 0.1415 for on and off kinetics, respectively. **i**–**n**, Spontaneous 5-HT and DA release. **i**, Representative pseudocolor images of the cumulative spontaneous transients during a 10-min recording. Similar results were observed for 7 slices. Scale bar, 100 μm. **j**, Representative time-lapse pseudocolor images, and $\Delta F/F_0$ traces of ROIs (10 μm in diameter) from the area indicated by the gray dashed rectangle in **i**. Scale bar, 20 μm. **k**, Number of transients in g5-HT3.0 and rDA3m fluorescence. Two-tailed paired *t*-tests, $P = 0.0226$. **l**, Distribution of the peak response of individual events. **m**, Example traces showing the rise and decay kinetics (t_{50}) of g5-HT3.0 and rDA3m (left), and the distribution of individual events (right). **n**, Distribution of the area of individual events. $n = 4$ slices from 3 mice in **c**,**d**,**g**,**h**; $n = 7$ slices of 3 mice in **k**; $n = 1060$ and 47 events for g5-HT3.0 and rDA3m, respectively, from 7 slices of 3 mice in **l**–**n**. Data are shown as mean ± s.e.m. in **c**,**d**,**g**,**h**,**k**, with the error bars or shaded regions indicating the s.e.m. $^*P < 0.05$, n.s., not significant.

https://doi.org/10.1038/s41592-024-02188-8

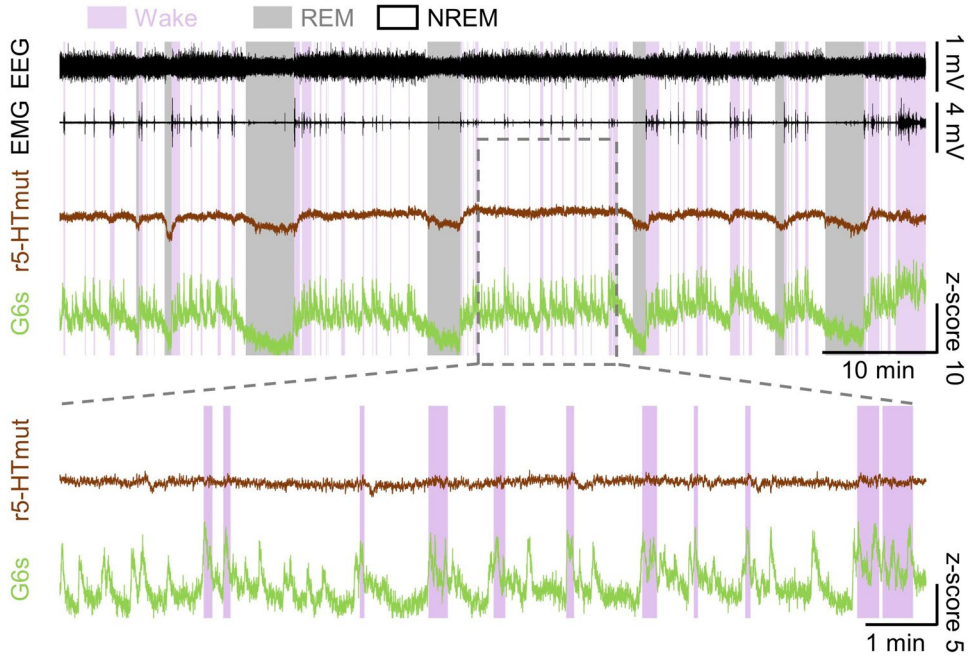

Extended Data Fig. 6 | Representative r5-HTmut and GCaMP6s signals during the sleep-wake cycle in freely moving mice. Representative r5-HTmut and GCaMP6s (G6s) traces in the mouse basal forebrain (BF) along with EEG and EMG recording during the spontaneous sleep-wake cycle.

https://doi.org/10.1038/s41592-024-02188-8

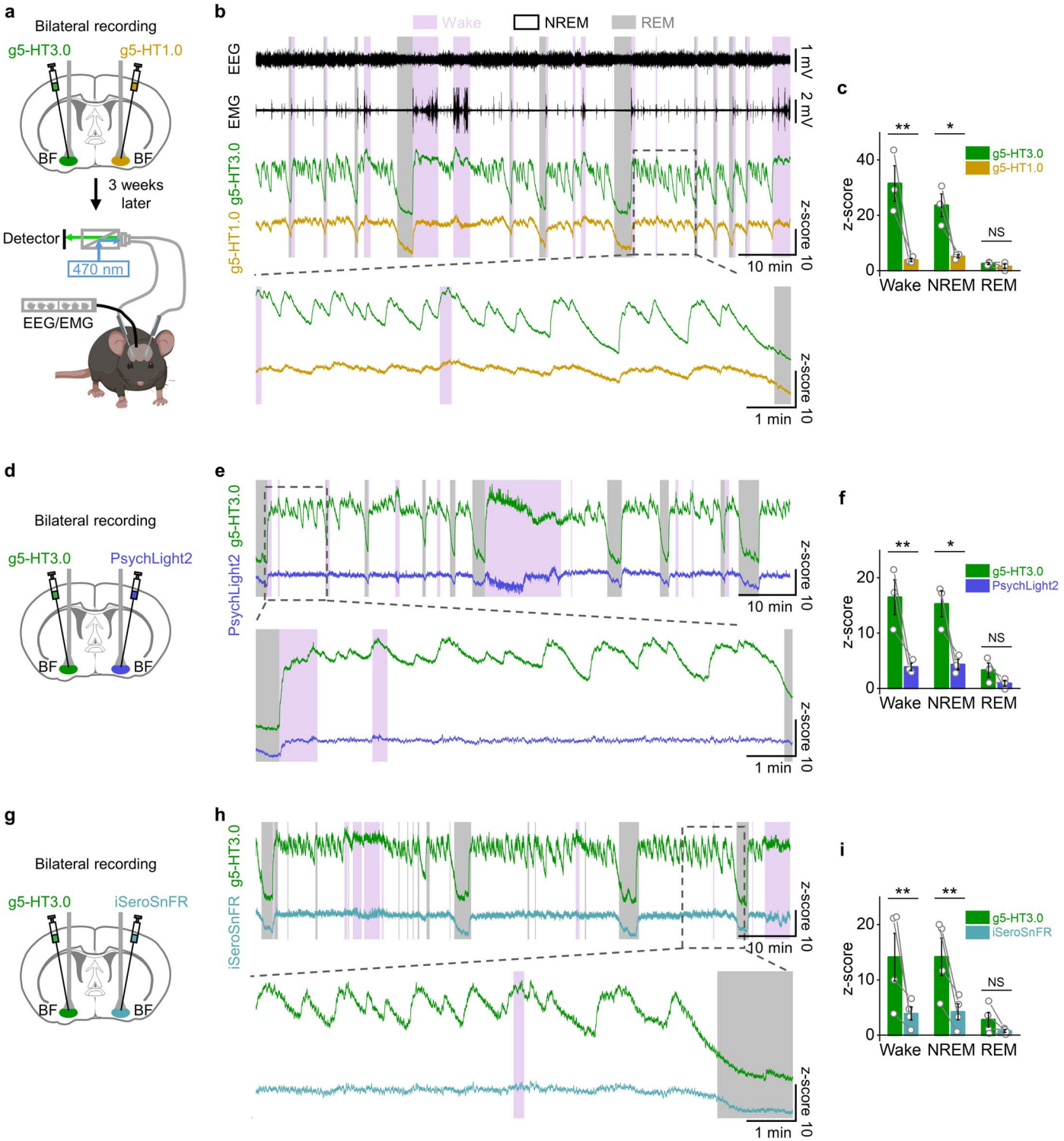

Extended Data Fig. 7 | Comparison of gGRAB$_{5\text{-}HT3.0}$ and other green 5-HT sensors during the sleep-wake cycle in freely moving mice. a, Schematic showing the setup of bilateral fiber-photometry recording of g5-HT3.0 and g5-HT1.0 during sleep-wake cycles in mice. **b**, Representative traces of simultaneous EEG, EMG, g5-HT3.0 and g5-HT1.0 recording during sleep-wake cycles in freely behaving mice. Pink shading, wake state; gray shading, REM sleep. **c**, Summary of averaged g5-HT3.0 and g5-HT1.0 signals in indicated sleep-wake states. $n = 3$ mice. Two-way repeated measures ANOVA followed by Tukey's multiple-comparison tests, $P = 0.0034$, 0.014 and 0.83 during wake, NREM and REM sleep state, respectively. **d**–**f**, Similar to **a**–**c**, except bilateral recording of g5-HT3.0 and PsychLight2, $n = 3$ mice in **f**. Two-way repeated measures ANOVA followed by Tukey's multiple-comparison tests, $P = 0.0066$, 0.011 and 0.38 during wake, NREM and REM sleep state, respectively. **g**–**i**, Similar to **a**–**c**, except bilateral recording of g5-HT3.0 and iSeroSnFR, $n = 4$ mice in **i**. Two-way repeated measures ANOVA followed by Tukey's multiple-comparison tests, $P = 0.0086$, 0.0095 and 0.47 during wake, NREM and REM sleep state, respectively. Data are shown as mean ± s.e.m. in **c**,**f**,**i**, with the error bars indicating the s.e.m. $^{*}P < 0.05$, $^{**}P < 0.01$, n.s., not significant.

https://doi.org/10.1038/s41592-024-02188-8

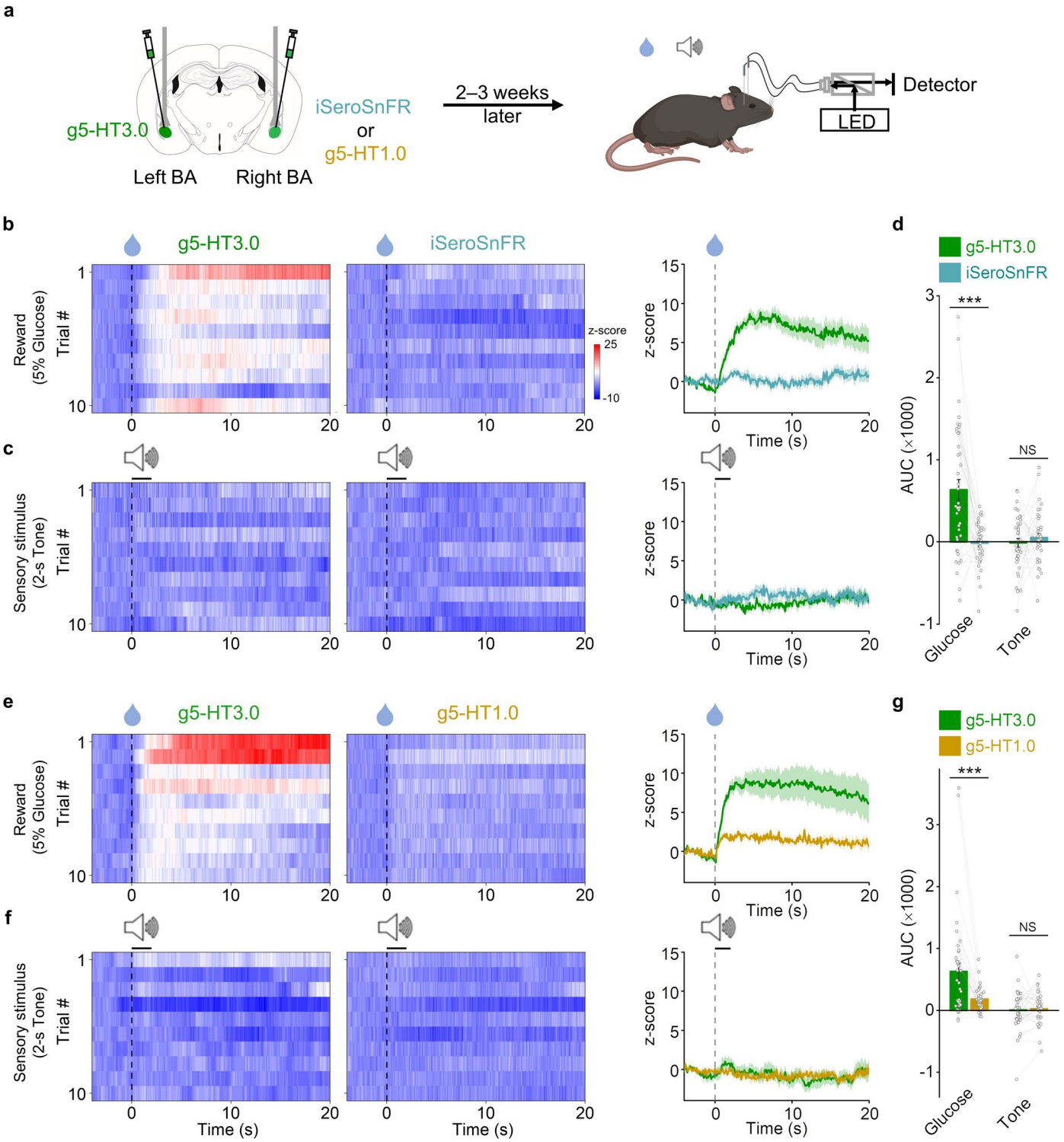

Extended Data Fig. 8 | Comparison of gGRAB$_{5\text{-}HT3.0}$ and other green 5-HT sensors during reward and tone delivery. a, Schematic illustrates the experimental design. **b**–**c**, Representative pseudocolor images (left) and averaged traces (right) of fluorescence signals (z-score) from g5-HT3.0 and iSeroSnFR in a mouse exposed to 5% glucose (**b**) or 2-s tone (**c**) conditions. The dashed line indicates the delivery of water or tone. **d**, Group analysis of the area under the curve (AUC) of fluorescence signals from g5-HT3.0 and iSeroSnFR in response to the application of 5% glucose or 2-s tone conditions. Two-tailed paired *t*-tests, $P = 2.4 \times 10^{-5}$ and 0.46 for glucose and tone, respectively. **e**–**g**, Representative pseudocolor images (left), averaged traces (right) and AUC group data (**g**) of fluorescence signals from g5-HT3.0 and g5-HT1.0 during exposure to 5% glucose (**e**) or 2-s (**f**) tone conditions, similar to panels **b**–**d**. Two-tailed paired *t*-tests in **g**, $P = 4.4 \times 10^{-4}$ and 0.632 for glucose and tone, respectively. $n = 40$ trials from 4 mice for each group. Data are shown as mean ± s.e.m. in **b**–**g**, with the error bars or shaded regions indicating the s.e.m. ***$P < 0.001$, n.s., not significant.

https://doi.org/10.1038/s41592-024-02188-8

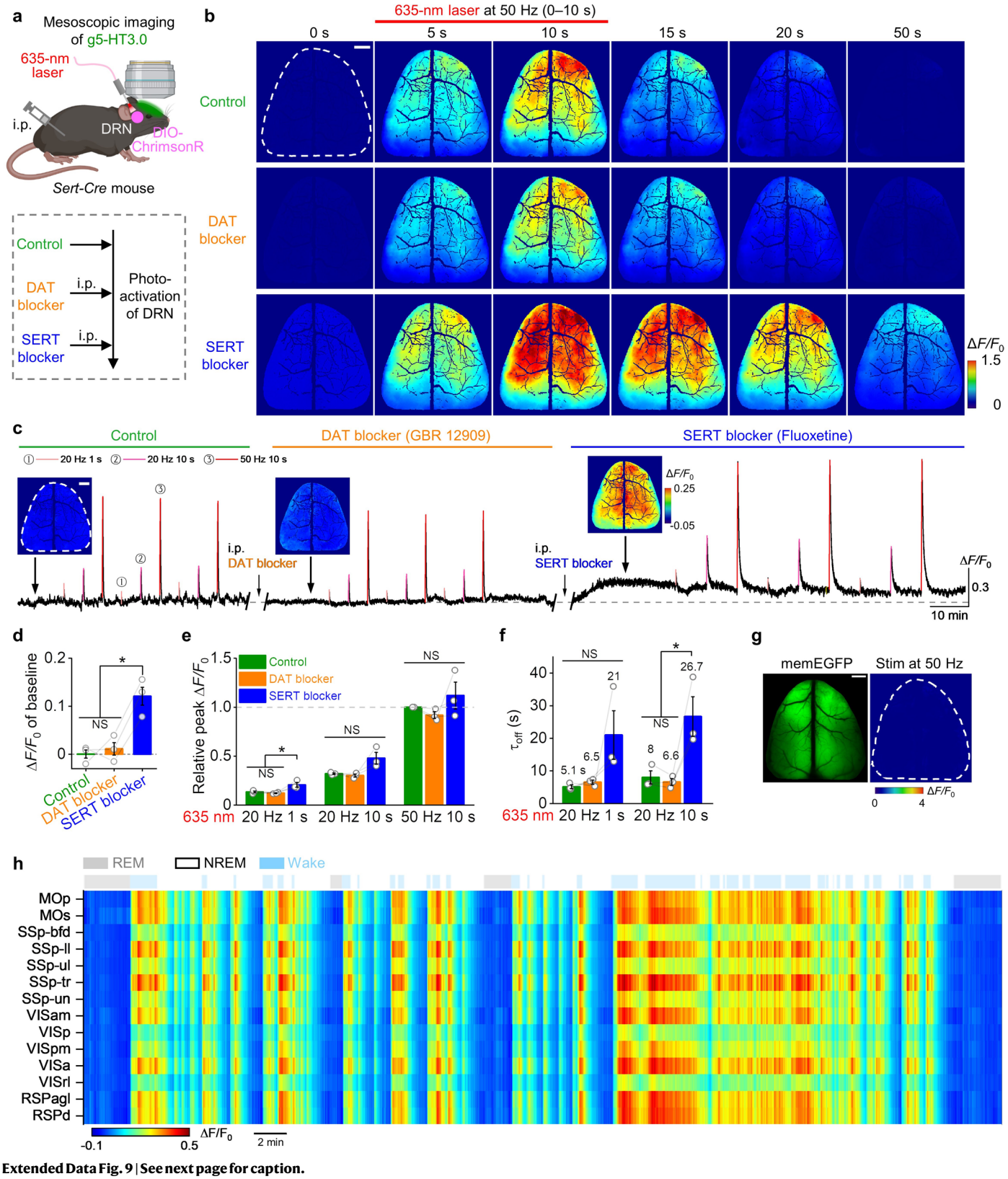

Extended Data Fig. 9 | See next page for caption.

https://doi.org/10.1038/s41592-024-02188-8

Extended Data Fig. 9 | gGRAB$_{5\text{-}HT3.0}$ reveals 5-HT dynamics in mouse dorsal cortex *in vivo*. **a**, Schematic depicting the protocol for mesoscopic imaging along with optogenetic activation of DRN with different drug treatments. **b**, Representative pseudocolor images in response to the 50 Hz 10 s optical stimulation of DRN with indicated treatments. Scale bar, 1 mm. **c**, Representative trace of g5-HT3.0 with indicated treatments, including the application of different drugs and activation of DRN using a 635-nm laser with different frequencies and durations. Insets above the trace are averaged images in the indicated baseline of different stages. Scale bar, 1 mm. **d**, Group data of averaged g5-HT3.0 baseline fluorescence changes under indicated treatments. $n = 3$ mice. One-way repeated measures ANOVA followed by Tukey's multiple-comparison tests, $F = 19.9$, $P = 0.047$, post hoc test: $P = 0.896$ for control versus DAT blocker, 0.016 for SERT blocker versus control and 0.022 for SERT blocker versus DAT blocker. **e**–**f**, Group summary of optical stimulation evoked peak response (**e**) and decay kinetics (**f**). $n = 3$ mice. One-way repeated measures ANOVA followed by Tukey's multiple-comparison tests. For relative peak $\Delta F/F_0$ in **e**, under 20 Hz 1 s stimulation, $F = 11.1$, $P = 0.023$, post hoc test: $P = 0.81$ for control versus DAT blocker, 0.043 for SERT blocker versus control and 0.026 for SERT blocker versus DAT blocker; under 20 Hz 10 s stimulation, $F = 6.67$, $P = 0.053$; under 50 Hz 10 s stimulation, $F = 1.39$, $P = 0.348$. For decay kinetics τ_{off} in **f**, under 20 Hz 1 s stimulation, $F = 4.06$, $P = 0.182$; under 20 Hz 10 s stimulation, $F = 16.78$, $P = 0.011$, post hoc test: $P = 0.932$ for control versus DAT blocker, 0.018 for SERT blocker versus control and 0.014 for SERT blocker versus DAT blocker. **g**, Representative images showing the memEGFP expression and response to the 50 Hz 10 s optical activation. Scale bar, 1 mm. **h**, Representative heatmap showing changes of g5-HT3.0 fluorescence in different brain regions during sleep-wake cycles. Gray shading, REM sleep; light blue shading, wake state. The dashed white outlines in **b**,**c**,**g** indicate the ROI. Data are shown as mean ± s.e.m. in **d**–**f**, with the error bars indicating the s.e.m. *$P < 0.05$, n.s., not significant.

https://doi.org/10.1038/s41592-024-02188-8

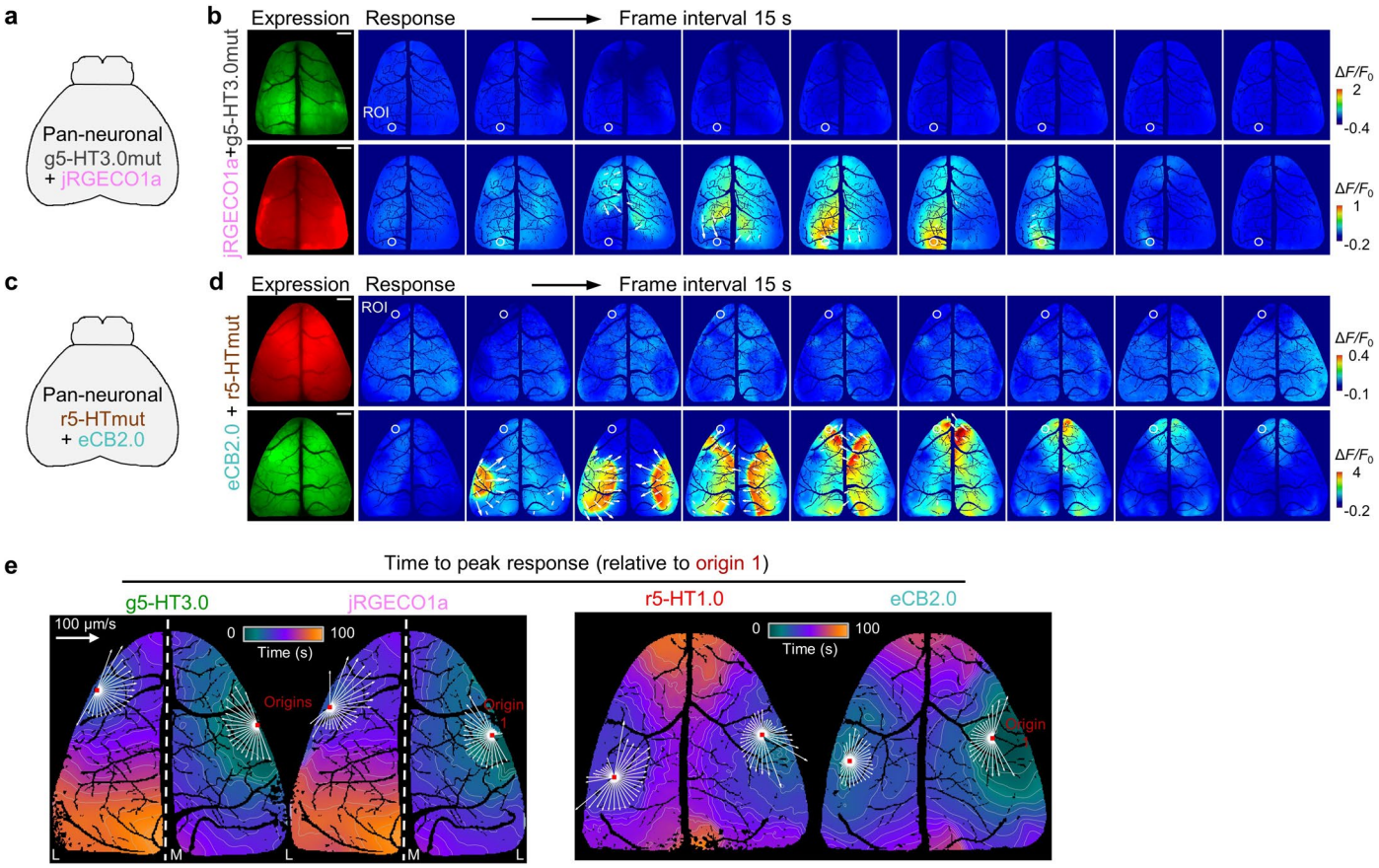

Extended Data Fig. 10 | Mesoscopic imaging of 5-HT, Ca^{2+} and eCB waves during seizures. a, Schematic showing the co-expression of g5-HT3.0mut and jRGECO1a in the mouse dorsal cortex. **b**, Representative images show fluorescence changes of g5-HT3.0mut (top) and jRGECO1a (bottom) during seizures. A ROI labeled with the white circle (500 μm in diameter) shows the maximum response regions of jRGECO1a, which corresponds to the trace in Fig. 5c. White arrows indicate the direction of wave propagation and the length of arrows indicates relative magnitudes of velocities. Scale bar, 1 mm. **c**–**d**, Similar to **a**–**b**, but co-expressing r5-HTmut and eCB2.0. The ROI shows the maximum response region of eCB2.0 and corresponds to the trace in Fig. 5e. **e**, Representative time to peak response maps of waves relative to the origin 1, monitored by different sensors. Red dots indicate origin locations of waves; white arrows indicate velocity vectors calculated based on the propagation distance and duration along the corresponding direction; L, lateral, M, medial; scale bar of speed, 100 μm/s.